Multiple Association in Ultra-Dense Networks

Mahmoud I. Kamel
Electrical and Computer Engineering
Concordia University
Montreal, Quebec, Canada.
Email: mah_kame@encs.concordia.ca

Walaa Hamouda
Electrical and Computer Engineering
Concordia University
Montreal, Quebec, Canada.
Email: hamouda@ece.concordia.ca

Amr M. Youssef
CIISE
Concordia University
Montreal, Quebec, Canada.
Email: youssef@ciise.concordia.ca

***Abstract*—The cell association is of a paramount effect on the operation of cellular network . In Ultra-Dense Networks (UDN), different types of small cells are deployed with extremely large densities. This comes with a great advantage of dense reuse of spectrum. In this paper, we investigate the downlink association of a given user equipment (UE) to multiple small cells, which we termed *multiple association*. In multiple association, a user connects to $M \geq 1$ small cells forming what we call *MultiCell*. Consequently, this overcomes the backhaul limitation of individual cells. Specifically, we derive the idle mode probability in the proposed setting, and based on that we derive an analytical expression for the average ergodic downlink rate of the link between the typical user and its jth nearest cell. Additionally, we exploit the aforementioned findings to study the area spectral efficiency in multiple association, and to investigate its relation to the main system parameters, namely: small cells density, users density, and *MultiCell* size M. We simulate the proposed model to assess the accuracy of the analytical results. Our results provide a mathematical framework, and pave the way to consider the association of a user to multiple small cells.**

I. Introduction

The ever-increasing growth in the mobile traffic, fueled by the popularization of powerful user mobile devices and bandwidth-hungry applications, requires a revolutionary growth in the network capacity [1]. The densification of wireless networks stems as a viable and long-term solution [2]. On one hand, the densification of small cells is cost-effective in the sense that more cells are deployed in a given hotspot, where more traffic would be generated. On the other hand, the deployment of more cells per unit area brings the cells much closer to the users which improves the link quality. Furthermore, deployment of more cells per unit area can be translated into more frequency reuse, and hence a better area spectral efficiency.

In Ultra-Dense Network (UDN) environments, small cells of low transmission power and small footprint are deployed with high densities [3]. The cells are deployed by the customers in their premises, or by the operators in the streets (e.g., on lampposts, trees, and walls) and hotspots (e.g., airports, metro/train stations, and markets). The UDN deployment scenarios introduces a different coverage environment; a given user would be in close proximity to many cells. The small cells in the neighborhood of a user could be dominant interferers or strong servers. This depends strongly on the association scheme and the coordination among the neighboring small cells.

One of the main challenges for the dense deployment of small cells is backhauling [4]. The promised radio interface capacity of the small cells might be bottlenecked by the wired or wireless backhaul capacity. To explain, the association of a user to a single small cell limits its maximum achievable data rate to the backhaul capacity of this cell. Moreover, the cloud-computing trend and the bandwidth-hungry applications accelerate the need to even higher data rates than what could be offered by a single cell. This motivates us to propose the multiple association scheme as a solution to distribute the traffic load of the user to multiple small cells in the user's neighborhood.

A. Related Work

The stochastic modeling of the spatial distribution of small cells has achieved significant results in the literature (e.g. see [5], [6]). The unplanned deployment of the access nodes reflects randomness in their placement. Hence, the positions of the small cells can be modeled as points in two- or three-dimensional Euclidean space, which is termed as a point process (PP) [7]. A common assumption in the recent research work is the fully-loaded network where each cell has at least one user in its coverage area [8], [9]. This assumption might be unrealistic in UDN environments which are characterized by the case where there are more cells than users. The lack of a clear definition of UDN in terms of the small cells density is addressed in [9], where the authors suggest a density over which a network is considered UDN ($\geq 10^3$ cells/km^2).

Only a small fraction of research work has considered UDN environments with a truly high density. The asymptotic relation between the density of base stations and the spectral efficiency is investigated in [10]. The success probability or equivalently the coverage probability and the area spectral efficiency in a UDN setting is studied in [8] assuming multiuser MIMO (Multi In Multi Out) cells, and in [9] considering line-of-sight (LOS) transmissions. The authors in [11] investigate the effect of multiple access on the user rate and the outage probability, and provide an upper bound for the access point density for a small rate outage probability. In [4], the authors present extensive simulations to analyze the potential gains of network densification along with the use of higher frequencies, and enhancements of spectral efficiency. However, a rigorous mathematical analysis is missing.

To the best of our knowledge, we are the first to propose

978-1-4799-6664-6/16/$31.00 ©2016 IEEE

multiple association in UDN environments. Motivated by the fundamental differences which are introduced by network densification, we model and analytically study the problem to provide a basic mathematical framework. It is important to realize that many aspects of the model can be further generalized and studied.

We organize the rest of the paper as follows. Section II describes the system model, and defines the user neighborhood. In section III, we derive the idle mode probability of the multiple association scheme. The average ergodic downlink rate is derived in section IV along with a discussion on area spectral efficiency. The numerical results are presented in section V, and finally we conclude the paper in section VI.

II. System Model

We consider the downlink of a small cell network environment. The positions of the small cells and mobile users form a realization of an independent homogenous Poisson Point Process (PPP) Φ_s with density λ_s, and Φ_u with density λ_u, respectively [5]. The UDN environments would be identified by the high density of the base stations per unit area with regard to the density of users. We assume a UDN is a network where $\lambda_s \gg \lambda_u$ [11]. Which in turn implies that many base stations are in idle mode due to the lack of connected users. We further assume that a base station in the idle mode is turned off to fully mitigate its interference.

This stochastic geometry representation of the network models the unplanned deployment of the small cells and the randomness of their positions, but with the advantage of increased tractability [6]. Without loss of generality, we develop the analysis considering a typical mobile user located at the origin [7]. The concept of a typical user in stochastic geometry refers to a user residing at the origin where the properties of the point process (PP) can be computed. In other words, the typical user is assumed to be a representative to all users.

We also assume that each small cell is equipped with a single antenna, and its transmission power is P_s. Furthermore, we consider a User Equipment (UE) equipped with a single antenna. The UE is assumed to connect to M small cells in its vicinity and to distribute the load amongst them. Thus, a *MultiCell* is formed from a group of the nearest M cells to a given user.

To model the radio propagation and the channel characteristics, we consider a standard power loss propagation model with pathloss exponent $\alpha > 2$. The multipath fading effect is modeled by a multiplicative channel gain h. Hence the received signal power at a user at a distance r_j from its jth nearest serving base station is $P_s h r_j^{-\alpha}$. We further assume that the fading channel follows a Rayleigh distribution with mean one, which implies that the channel gain h is exponentially distributed with mean one, hence $h \sim exp(1)$.

Figure 1 illustrates a typical user at the origin in a UDN environment. The set of small cells that a user u connects to them to form a *MultiCell* $\mathcal{V}_u$ is a subset of all BSs in its *neighborhood* $\mathcal{N}_u$, which is defined as follows:

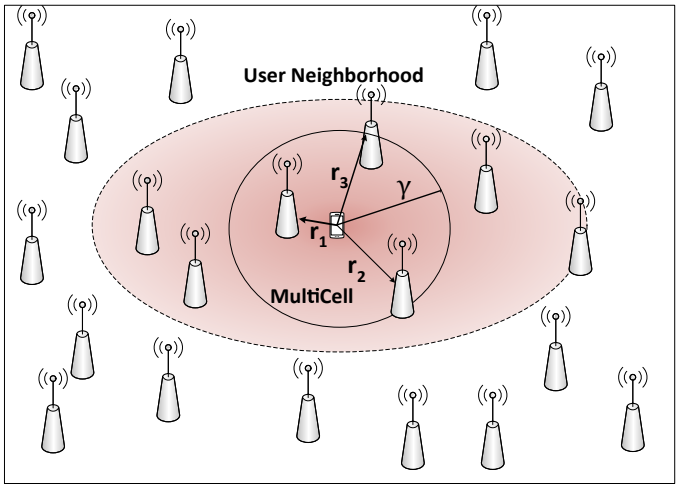

Fig. 1: The user neighborhood is the cells which are in close proximity to a given user, this proximity is characterized by the average received signal strength threshold ρ. The *MultiCell* is a subset of the user neighborhood, the user connects to the nearest M cells to form its *MultiCell*

Definition 1. *The user neighborhood $\mathcal{N}_u$ for a given user u is the set of small cells where the average received signal strength from a BS $s \in \mathcal{N}_u$ is above a given threshold ρ.*

In other words, the user neighborhood is the set of small cells which are in close proximity to this user, and hence they are either dominant interferers or potential servers. Since the positions of the small cells follows a PPP, the probability of finding n nodes in a disc of radius γ and centered at the origin (where the typical user resides) is given by the Poisson distribution [5]

$$P[|\mathcal{N}_u| = n] = \frac{(\pi\gamma^2\lambda_s)^n}{n!} e^{-\pi\gamma^2\lambda_s}. \tag{1}$$

Moreover, the expectation of the neighborhood size $N = |\mathcal{N}_u|$ is given by:

$$\mathbb{E}[N] = \pi\gamma^2\lambda_s, \tag{2}$$

and the radius of the user neighborhood γ is thus the distance from the typical user's position (the origin) to a point which if it is occupied by a small cell, the average received signal at the origin is ρ.

Lemma 1. *Based on the definition of the neighborhood radius γ, it is given by*

$$\gamma = (\frac{\rho}{P_s})^{-\frac{1}{\alpha}}, \tag{3}$$

yielding to

$$\mathbb{E}[N] = \lambda_s \pi (\frac{\rho}{P_s})^{-\frac{2}{\alpha}}. \tag{4}$$

Proof. The threshold ρ is defined as the average received signal power at the origin from a base station at a distance γ, i.e.,

$$\rho = \mathbb{E}_h[P_s h \gamma^{-\alpha}] = P_s \gamma^{-\alpha} \mathbb{E}_h[h],$$

and since the channel fading gain h follows an exponential distribution with mean one, therefore

$$\rho = P_s \gamma^{-\alpha},$$

and hence

$$\gamma = (\frac{\rho}{P_s})^{-\frac{1}{\alpha}},$$

and (4) follows simply from substitution in (2) □

We assume that the small cells in the *MultiCell* are cooperating perfectly to fully mitigate the interference inside the *MultiCell*. In other words, the user connects to the small cells in its *MultiCell* on orthogonal frequencies, and the bandwidth is then reused in another *MultiCell* of a different user. This introduces a new frequency reuse scheme, where the full bandwidth is exploited inside a *MultiCell*, and then reused in a neighboring *MultiCell*. Also, it is important to mention that the *MultiCell* radius is the distance from the user to its Mth nearest cell. Henceforth, we assume that the neighbourhood of a given user shrinks to its *MultiCell*. In other words, the user connects to the nearest M small cells in its neighbourhood and drops out whatever left in the set $\mathcal{N}_u$. A direct interpretation of this assumption is that the radius of the *MultiCell* is the same as the radius of the neighbourhood, i.e., γ.

III. Idle Mode Probability

In UDN, the density of the cells is much greater than the density of the users, i.e. $\lambda_s \gg \lambda_u$. As a direct consequence of this property, most of the small cells are lightly loaded or inactive. A small cell is turned off if there is no users in its coverage area, this is known as idle mode capabilities [13], [4].

The probability for a small cell to be in idle mode, p_o, is thus of a special importance. Turning off an idle base station results in the mitigation of its interference towards other cells. The base station is turned off, according to the system model in section II, if it is not a cell in *MultiCell* or equivalently if no users connect to it. The probability mass function (PMF) of the number of users, X, in the coverage area of a *MultiCell* is relevant to the computation of the idle mode probability, and it is given in the following lemma.

Lemma 2. *Consider the random variable X which stands for the number of users in the coverage area of an arbitrary* MultiCell*. The* MultiCell *is formed from a set of small cells and X users are randomly placed in the aggregate area of their respective Voronoi cells. The PMF of the number X, averaged over the statistics of the point process Φ_s of the small cells is given by*

$$P[X = x] = \frac{\Gamma(x + 3.5)(3.5\frac{\kappa}{M})^{3.5}}{\Gamma(3.5)x!(1 + 3.5\frac{\kappa}{M})^{x+3.5}}, \quad (5)$$

where $\kappa \triangleq \lambda_s/\lambda_u$ is the densification ratio of the small cell network, and $\Gamma(n) = \int_0^\infty t^n e^{-t} dt$ is the gamma function.

Proof. In the multiple association scheme, a user connects to the nearest M cells in its neighborhood. Therefore, we can replace the typical UE by an equivalent M UEs each supports a single association and uniformly distributed in the aggregate area of the cells forming the *MultiCell*. The density of the equivalent single association users is $M\lambda_u$. Following similar steps as in the proof of Lemma (1) in [12] we arrive at (5) completing the proof. □

The probability $p_o = P[X = 0]$ is then given by:

$$p_o = \left(\frac{3.5\kappa}{M + 3.5\kappa}\right)^{3.5}. \quad (6)$$

It is interesting to note that the expression of the idle mode probability in (6) for the multiple association case collapses to the expression of the idle probability in case of single association by setting $M = 1$. Consequently, the idle mode probability derived in Lemma 2 provides the general expression for the idle mode probability assuming that the UE is equipped with the capability to connect to M cells.

Henceforth, we use the idle mode probability to perform an independent thinning of the small cells point process. Since we assume that a small cell in idle mode is turned off to fully mitigate its interference, therefore we account only for the interference generated from the active small cells in the computation of the interference. The interfering small cells which are active and transmit at the same time with the tagged base stations of the typical user form a thinned version of the original PPP [7]. In the p-thinning of a PPP Ψ with intensity λ, we form another PPP Ψ_{th} with intensity $p\lambda$ where $\Psi_{th} \subset \Psi$. The p-thinning means that a given point is deleted from a PP with a probability $1 - p$.

IV. Multiple Association Average Downlink Rate and Area Spectral Efficiency

In this section we develop an analytical expression for the average downlink rate of the typical user while connecting to a small cell $j \in \mathcal{V}_u$, or equivalently connecting to a small cell in its *MultiCell*. Also, we study the Area Spectral Efficiency (ASE) in the multiple association setting. In particular, we show the relation between the ASE and the main system parameters, namely: the small cells density, the user density, and the *MultiCell* size M.

A. Average Downlink Rate

The signal to interference-plus-noise ratio (SINR) in the downlink of a mobile user at a random distance r_j from its jth nearest small cell can be expressed as

$$\texttt{SINR}_j = \frac{P_s h_j r_j^{-\alpha}}{\sigma^2 + I_o}, \quad (7)$$

where I_o is the cumulative interference from all active small cells forming the thinned PPP $\Phi_\gamma \subset \Phi_s$. The interfering small cells are outside the *MultiCell* of the typical user at a distance r_i and have fading gain g_i, which is given by

$$I_o = \sum_{i \in \Phi_\gamma / \mathcal{V}_u} P_s g_i r_i^{-\alpha}, \quad (8)$$

where the intensity of the thinned PPP Φ_γ is $(1 - p_o)\lambda_s$.

The definition of the interference term implies that there exists a coordination between the small cells of the *MultiCell* of a given user to perfectly mitigate the interference. The interference is a standard shot noise [16] created by a PPP of intensity $(1-p_o)\lambda_s$ outside a disc centered at the typical user and of radius γ, i.e. the interference comes from outside the *MultiCell* of the typical user resides at the origin.

Let R_j denote the achieved downlink rate by the typical user connected to its jth nearest small cell. Then we have

$$R_j = log(1+\texttt{SINR}_j). \tag{9}$$

Also let $\bar{R}_j$ denote the average ergodic downlink rate of the corresponding connection, i.e., $\bar{R}_j = \mathbb{E}[R_j]$

In the following theorem we compute the average ergodic downlink rate of a typical user in the downlink while connected to a small cell in its *MultiCell*.

Theorem 1. *The average ergodic downlink rate of the typical user while connected to the jth base station in a* MultiCell *in the UDN environment described in the system model of section II is given by*

$$\bar{R}_j = \int_{r>0}\left(\int_{t>0} e^{-\frac{\sigma^2 r^\alpha}{P_s}(e^t-1)}\mathcal{L}_{I_o}\left(\frac{r^\alpha(e^t-1)}{P_s}\right)\mathrm{d}t\right) f_j(r)\mathrm{d}r, \tag{10}$$

where

$$\mathcal{L}_{I_o}\left(\frac{r^\alpha(e^t-1)}{P_s}\right) = \exp\left(-\pi(1-p_o)\lambda_s r^2(e^t-1)^{2/\alpha}\int_{\frac{\gamma^2}{r^2}(e^t-1)^{-2/\alpha}}^{\infty}\frac{1}{1+u^{\alpha/2}}\mathrm{d}u\right), \tag{11}$$

and $f_j(r)$ is the probability density function of the distance r to the jth nearest small cell from the typical user at the origin, and is given by [5]

$$f_j(r) = \frac{2}{\Gamma(j)}(\lambda_s\pi)^j r^{2j-1}e^{(-\lambda_s\pi r^2)}. \tag{12}$$

Proof. We begin by referring to the definition of the average downlink rate of the connection of the typical user to the jth nearest cell $\bar{R}_j = \mathbb{E}[R_j] = \mathbb{E}[log(1+\texttt{SINR}_j)]$. Averaging the rate over the statistics of the PPP Φ_s and the fading distribution, it follows that

$$\begin{aligned}
\bar{R}_j &= \mathbb{E}_{sinr}[\log(1+\texttt{SINR}_j)]\\
&= \mathbb{E}_r\left[\mathbb{E}_{sinr}\left[\log(1+\texttt{SINR}_j)|r\right]\right]\\
&\overset{(a)}{=} \mathbb{E}_r\left[\int_{t>0}\mathbb{P}\left(\log(1+\texttt{SINR}_j)>t\right)\mathrm{d}t|r\right]\\
&\overset{(b)}{=} \int_{r>0}\left(\int_{t>0}\mathbb{P}\left(\log(1+\texttt{SINR}_j)>t\right)\mathrm{d}t\right)f_j(r)\mathrm{d}r\\
&= \int_{r>0}\left(\int_{t>0}\mathbb{P}\left[\log\left(1+\frac{P_s h_j r^{-\alpha}}{\sigma^2+I_o}\right)>t\right]\mathrm{d}t\right)f_j(r)\mathrm{d}r\\
&\overset{(c)}{=} \int_{r>0}\left(\int_{t>0}\mathbb{P}\left[h>r^\alpha\left(\frac{\sigma^2+I_o}{P_s}\right)(e^t-1)\right]\mathrm{d}t\right)f_j(r)\mathrm{d}r
\end{aligned}, \tag{13}$$

The inner probability can be evaluated as [15]

$$\mathbb{P}\left[h>r^\alpha\left(\frac{\sigma^2+I_o}{P_s}\right)(e^t-1)\right] = e^{-\frac{\sigma^2 r^\alpha}{P_s}(e^t-1)}\mathcal{L}_{I_o}\left(\frac{r^\alpha(e^t-1)}{P_s}\right), \tag{14}$$

where $\mathcal{L}_{I_o}(s)$ is the Laplace transform of the interference random variable term I_o evaluated at s. Step (a) follows from the fact that for a positive random variable X, $\mathbb{E}[X] = \int_{t>0}\mathbb{P}(X>t)dt$, and in step (b) we employ the pdf of the distance to the jth nearest small cell. In step (c), we use the assumption that the channel fading of the connections to the small cells inside the *MultiCell* are identically distributed. Finally, in (14) we use the assumption that the fading channels follow exponential distribution of mean one, i.e. $h\sim exp(1)$.

To further simplify the average rate expression, we use the definition of the Laplace transform

$$\begin{aligned}
\mathcal{L}_{I_o}(s) &= \mathbb{E}_{I_o}[e^{-sI_o}]\\
&= \mathbb{E}_{\Phi_\gamma,\{g_i\}}\left[\exp\left(-s\sum_{i\in\Phi_\gamma/\mathcal{N}_u}P_s g_i r_i^{-\alpha}\right)\right]\\
&= \mathbb{E}_{\Phi_\gamma,\{g_i\}}\left[\prod_{i\in\Phi_\gamma/\mathcal{N}_u}\exp\left(-sP_s g_i r_i^{-\alpha}\right)\right]\\
&\overset{(a)}{=} \mathbb{E}_{\Phi_\gamma}\left[\prod_{i\in\Phi_\gamma/\mathcal{N}_u}\mathbb{E}_g\left[\exp\left(-sP_s g r_i^{-\alpha}\right)\right]\right]\\
&\overset{(b)}{=} \exp\left(-2\pi\lambda_\gamma\int_\gamma^\infty\left(1-\mathbb{E}_g\left[\exp\left(-sP_s g\nu^{-\alpha}\right)\right]\right)\nu\mathrm{d}\nu\right)\\
&= \exp\left(-2\pi(1-p_o)\lambda_s\int_\gamma^\infty\left(1-\mathbb{E}_g\left[\exp\left(-sP_s g\nu^{-\alpha}\right)\right]\right)\nu\mathrm{d}\nu\right).
\end{aligned} \tag{15}$$

We assume that the fading channel gains g_i of the potential interferers outside the *MultiCell* are i.i.d., and they are independent from the corresponding point process Φ_γ. This gives the support for step (a). In step (b) we applied Campbell's theorem for the probability generating functional (PGFL) of the PPP [5]. The last step follows from the relation between the original process Φ_s and the thinned version Φ_γ to account for the idle mode probability of the potential interferers. The integration limits are set from γ to ∞ since we consider that the nearest interferer would be at the edge of the *MultiCell*, i.e., at a distance γ from the typical user.

To proceed, we average over the statistics of the fading channel g

$$\begin{aligned}
\mathbb{E}_g\left[\exp\left(-sP_s g\nu^{-\alpha}\right)\right] &= \int_0^\infty e^{-sP_s g\nu^{-\alpha}}f_G(g)\mathrm{d}g\\
&\overset{(a)}{=} \int_0^\infty e^{-sP_s g\nu^{-\alpha}}e^{-g}\mathrm{d}g = \int_0^\infty e^{-g(1+sP_s g\nu^{-\alpha})}\mathrm{d}g\\
&= \frac{1}{1+sP_s\nu^{-\alpha}},
\end{aligned} \tag{16}$$

where $f_G(g)$ is the PDF of the fading channel gain and in step (a) we consider the assumption of exponential fading with mean one.

Returning to (15), we proceed by substitution of $s = \frac{r^\alpha(e^t-1)}{P_s}$ and by simple manipulation we obtain

$$\mathcal{L}_{I_o}\left(\frac{r^\alpha(e^t-1)}{P_s}\right) = \exp\left(-2\pi(1-p_o)\lambda_s \int_\gamma^\infty \frac{1}{1+\left(\frac{\nu}{r}(e^t-1)^{\frac{-1}{\alpha}}\right)^\alpha}\nu \mathrm{d}\nu\right) = \exp\left(-\pi(1-p_o)\lambda_s r^2(e^t-1)^{2/\alpha}\int_{\frac{\gamma^2}{r^2}(e^t-1)^{-2/\alpha}}^\infty \frac{1}{1+u^{\alpha/2}}\,\mathrm{d}u\right) \quad (17)$$

The last step follows from the change of variables $u = \left(\frac{\nu}{r}(e^t-1)^{\frac{-1}{\alpha}}\right)^2$ which completes the proof. □

B. Area Spectral Efficiency

We use the area spectral efficiency (ASE) as the performance metric to account for the network capacity. The ASE is defined as the number of transmitted bits per second (bps) per Hz. per unit area. The interpretation of this definition in the context of multiple association is the sum of the average ergodic downlink rate in a *MultiCell* multiplied by the number of Multicells per unit area. Since each user forms a *MultiCell* by multiple association to many cells in its vicinity; the *MultiCell* density is the same as the users density. Hence, the ASE is defined as

$$ASE \triangleq \lambda_u \sum_{j=1}^{M} \bar{R}_j. \quad (18)$$

We assume that the Multicells are non overlapping, i.e., there is no small cell that serves two users simultaneously. Accordingly, a given small cell in the multiple association scenario is either in idle mode or serves at most one user. Recall that in UDN environments there is a fundamental difference from traditional networks, the density of cells is larger than the density of users.

V. Numerical Results

In this section , We assess the accuracy of our analytical results when compared to simulations. We realize a PPP in a square with area of 1 km^2. We generate 1000 spatial realizations of the PPP. The channel variation is simulated by a realization of 100 time slots drawn from an exponential random variable with a mean one. We assume $\alpha = 4$, and $\sigma^2 = 0$ (i.e. no noise) in all simulations. Additionally, we scale the units of the average downlink rate and the area spectral efficiency in the numerical results. Although the analysis is performed assuming a natural logarithm in (9) which corresponds to the unit of nats/sec/Hz, but a simple transformation to the unit of bit/sec/Hz is applied (1 nat/sec/Hz = 1.44 bps/Hz).

A. Idle Mode Probability

Figure 2 shows the idle mode probability versus the densification ratio for different *MultiCell* size. The simulation results are perfectly matched with the analytical expression. The probability of idle mode base stations in case of multiple association is smaller than the case of single association. This behavior is intuitive. In multiple association, more small cells are activated to form the *MultiCell* of a given user; hence, less base stations are in the idle mode. However, the probability of idle mode for different *MultiCell* size converges to almost the same value at extremely large small cell density. This is explained by approximating the idle mode probability in (6) to $p_o \approx 1 - \frac{M\lambda_u}{\lambda_s}$.

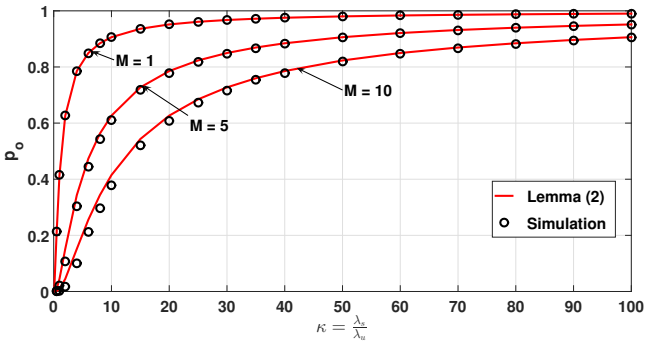

Fig. 2: Idle mode probability versus the densification ratio for different *MultiCell* size M.

B. Average Ergodic Downlink Rate

Figure 3 depicts the average ergodic downlink rate versus the small cell density for the connection of a typical user to the first, second, and third nearest small cells. The results show that the average ergodic downlink rate monotonically increases with higher small cell density, however the gains are diminishing. The difference between the average downlink rate of the link to the first and second nearest small cell, or the second and third nearest small cell is independent of the cell density in dense scenarios. Also, the loss in the average downlink rate due to connecting to farther cells is decreasing with the index of the small cell (first, second, third, etc.).

C. Area Spectral Efficiency

Figure 4 illustrates the area spectral efficiency versus small cells density for different *MultiCell* size. The results show a higher ASE for higher *MultiCell* sizes. This is due to the increase of the number of connections per unit area which significantly improves the area spectral efficiency. Moreover, the ASE in case of single association ($M = 1$) is invariant for larger small cells density. This is intuitive, the number of connections does not change with higher small cells density, and the gain in average downlink rate is diminishing. However, in multiple association the ASE is increasing with the small cells density. This would be explained by recalling that higher small cells density brings the cells closer to the user.

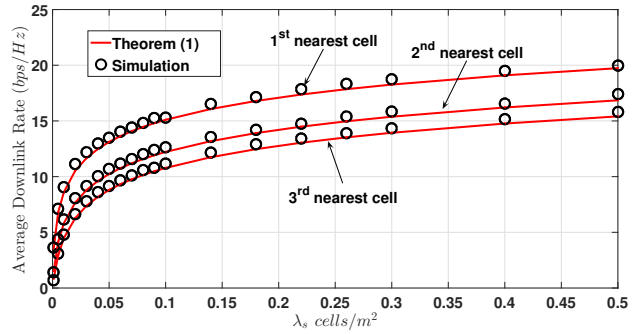

Fig. 3: Average downlink rate for different small cell density of the connections of the typical user with the first, second, and third nearest cells. ($\rho = -40$ dBm, $P_s = 20$ dBm, $\lambda_u = 300$ users/Km^2

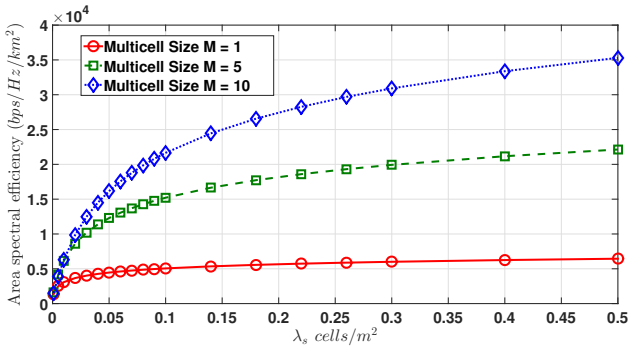

Fig. 4: Area spectral efficiency versus small cell density for different *MultiCell* size ($\lambda_u = 300$ users/Km^2, $P_s = 20$ dBm).

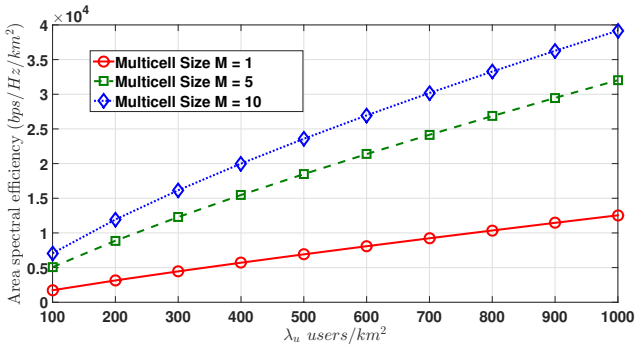

Fig. 5: Area spectral efficiency versus user density for different *MultiCell* size ($\lambda_s = 0.05$ cells/Km^2, $P_s = 20$ dBm).

Accordingly, the link quality to the nearest M cells improves significantly with higher densities of the small cells.

The effect of higher user density on the ASE is shown in Figure 5. The area spectral efficiency is increasing with the user density. In multiple association, the number of connections increases linearly with the user density. As a result, the ASE improves significantly with higher user density for larger *MultiCell* sizes.

VI. Conclusion

In this paper we proposed the multiple association scheme, where a user connects to many cells in its vicinity to form a *MultiCell*. In a multiple association scenario, the user distributes its traffic amongst many cells breaking the backhaul limitation of individual cells and aggregating higher data rates. We derived the idle mode probability in the multiple association setting and we developed an analytical expression for the average ergodic capacity of different connections in the *MultiCell*. Moreover, we defined the area spectral efficiency in multiple association scenario. The idle mode probability is shown to be less in larger *MultiCell* sizes. This is due activation of more cells in the user neighborhood. The results also show that the ASE in case of multiple association improves significantly with larger *MultiCell* sizes, and with higher user densities. Further extensions to this investigation might include the consideration of multi-slope radio propagation models. Also, the consideration of multiuser MIMO would be an important extension.

References

[1] Cisco, Cisco visual network index: Global mobile traffic forecast update 2014-2019. White paper (May 2015)

[2] I. Hwang, B. Song, and S. Soliman," A holistic view on hyper-dense heterogeneous and small cell networks," *IEEE Commun. Mag.*, vol. 51, no. 6, pp. 20–27, Jun. 2013.

[3] N. Bhushan et al. "Network densification: the dominant theme for wireless evolution into 5G," *IEEE Commun. Mag.*, vol. 52, no. 2, pp. 8289, Feb. 2014.

[4] D. Lopez-Perez, M. Ding, H. Claussen, and A. H. Jafari, "Towards 1 Gbps/UE in cellular systems: Understanding ultra-dense small cell deployments," to appear in *IEEE Commun. Surveys Tuts*, [online] available at http://arxiv.org/abs/1503.03912. 2015

[5] M. Haenggi, Stochastic geometry for wireless networks, Cambridge Univ. Press, 2012.

[6] H. ElSawy et al., "Stochastic geometry for modeling, analysis, and design of multi-tier and cognitive cellular wireless networks: A survey," *IEEE Commun. Surveys Tuts*, vol. 5, 2013, pp. 996–1019. Jun. 2013

[7] D. Stoyan, W. S. Kendall, and J. Mecke, Stochastic geometry and its applications, 2nd edition. John Wiley and Sons, 1995.

[8] C. Li, J. Zhang, S. Song, and K. B. Letaief, "Analysis of area spectral efficiency and link reliability in multiuser MIMO HetNets," *in Proc. IEEE Int. Conf. on Commun.* (ICC 2015), London, UK, Jun. 2015.

[9] M. Ding, D. Lopez-Perez, G. Mao, P. Wang, and Z. Lin, "Will the area spectral efficiency monotonically grow as small cells go dense?," [online] available at: http://arxiv.org/abs/1505.01920, 2015.

[10] J. Park, S.-L. Kim, and J. Zander, "Asymptotic behavior of ultra-dense cellular networks and its economic impact," *in Proc. IEEE Global Commun. Conf.* (GLOBECOM 2014), Austin, TX, United Sates, Dec. 2014.

[11] S. Stefanatos, A. Alexious, "Access point density and bandwidth partitioning in ultra-dense wireless network", *IEEE Trans. Commun.*, vol. 62, no. 9, pp. 3376–3384, Aug. 2014

[12] S. M. Yu and S.-L. Kim, "Downlink capacity and base station density in cellular networks," *in Proc. IEEE Int. Symp. WiOpt*, May 2013, pp. 119–124.

[13] H. Claussen, I. Ashraf, and L. T. W. Ho, "Dynamic idle mode procedures for femtocells," Bell Labs Tech. J., vol. 15, pp. 95–116, 2010.

[14] S. Lee and K. Huang, "Coverage and economy in cellular networks with many base stations," *IEEE Commun. Lett.*, vol. 16, no. 7, pp. 1038–1040, Jul. 2012.

[15] J. G. Andrews, F. Baccelli, and R. K. Ganti, "A tractable approach to coverage and rate in cellular networks," *IEEE Trans. Commun.*, vol. 59, no. 11, pp. 3122–3134, Nov. 2011.

[16] S. B. Lowen and M. C. Teich, "Power-law shot noise," *IEEE Trans. Inf. Theory*, vol. 36, no. 6, pp. 1302–1318, Nov. 1990.